Damping Control Combined to Output Stage for a Multi-Modular Matrix Converter

Hiroki Takahashi
Dept. of Electrical, Electronics and Information Engineering
Nagaoka University of Technology
Nagaoka Niigata, Japan
thiroki@stn.nagaokaut.ac.jp

Jun-ichi Itoh
Dept. of Electrical, Electronics and Information Engineering
Nagaoka University of Technology
Nagaoka Niigata, Japan
itoh@vos.nagaokaut.ac.jp

***Abstract*— This paper discusses a damping control that is applied for multi-modular matrix converters to suppress the oscillation by the LC resonance caused from the input filter. The multi-modular matrix converter connects a multiple winding transformer with several modules, which each module is consisting of a three-phase to single-phase matrix converter. It is found that the multi-modular matrix converter has the resonance problem between the leakage inductance of the transformer and filter capacitors. In this paper, the damping control that is combined to the output current control of the multi-modular matrix converter is implemented to suppress the resonance and to achieve better input current quality. The proposed damping control can divert the output current sensors for ACR (Auto Current Regulator), which is generally used in adjustable speed drive system of a motor, and additional sensors are not required. From the experimental results, the proposed damping control improves the input current THD by 72.1 %.**

I. INTRODUCTION

Recently, matrix converters have attracted a lot of attentions among the researchers because this converter has no DC energy buffer such as bulky electrolytic capacitors [1]-[7]. Matrix converters promise to achieve higher efficiency, smaller size and longer life-time compared to the conventional BTB (Back to Back) system which consists of a PWM (Pulse Width Modulation) rectifier and a PWM inverter. In addition, matrix converters achieve bidirectional power flow, unity input power factor, and sinusoidal input and output waveforms.

In order to utilize these advantages of matrix converters for high power applications, such as the wind turbines, pumps and blowers, the multi-modular matrix converters that consist of several modules of three-phase to single-phase matrix converter and a multiple winding transformer are investigated [8]-[10]. The multiple winding transformer is placed between a power grid and matrix converter modules, and output terminals of each module are connected in series or parallel in order to provide high voltage or high power. The advantages of this modular structure with the multiple winding transformer are following: 1) the circuit structure, especially placement of devices in the modules are simple; 2) special modulation schemes to prevent the interference between the connected modules are not required because the transformer can isolate each module. Consequently, high power conversion systems employing matrix converter topologies can be designed and composed easily with the conventional modulation schemes.

The multi-modular matrix converter requires LC filters in the input side to eliminate the harmonic current due to the switching operation and to assist in commutation similarly to the general matrix converters. Besides, the multi-modular matrix converter uses the filter capacitors only because the leakage inductance of the transformer can be treated as the filter reactors. That is, filter reactors are not required. Nevertheless, if the LC resonance occurs between the leakage inductance and the input filter capacitors in the matrix converter modules, the resonance can result in substantial distortions in the input current. A general solution to the problem of resonance in a standard matrix converter is to connect damping resistors in parallel with the input filter reactors [11]. However, in the multi-modular matrix converter, the damping resistors cannot be connected in parallel with the leakage inductance of the transformer, practically.

One of other solution to suppress the resonance is to connect the damping resistors in series with the input filter capacitors in the modules. However, this method results in more losses in the damping resistors due to harmonic current caused by switching operation in comparison with the former method. Hence, the solution using a special control to suppress the resonance is necessary.

In the controls to suppress the filter resonance, active damping controls for current source converters and general matrix converters have been proposed [12]-[16]. These methods suppress the resonance with virtual damping resistors in parallel with filter capacitors based on the input current control. On the other hand, the damping control combined with the output current control of a standard matrix converter was suggested [17]. This method can achieve the resonant suppression and output current control at a same time, and

also control input current with open-loop. However, the damping control suitable for multi-modular matrix converters and its validity have not been clarified. In addition, the damping controls which have been discussed in [12]-[16] generally require high accuracy and high speed response voltage sensors connected to the filter capacitors of every matrix converter module.

In this paper, the damping control that is implemented into the output stage of the multi-modular matrix converter is proposed. The proposed damping control can suppress the filter resonance and also divert the output current sensors for ACR (Auto Current Regulator), which is generally used in adjustable speed drive system of a motor, instead of using high speed response voltage sensors on the input stage. Firstly, the mechanism of the filter resonance is clarified in this paper. Second, the proposed damping control is discussed with the control block diagram. Finally, the validity of the proposed damping control for the multi-modular matrix converter is confirmed by simulation and experimental results.

II. MULTI-MODULAR MATRIX CONVERTER

A. System Configuration

Fig. 1 shows the system configuration of a series multi-modular matrix converter with nine modules as shown in [8]-[10]. The series topology can output 7-level high voltage which results in low harmonic components. A multiple winding transformer is located between the power source and matrix converter modules. The transformer cancels the low order harmonics in the primary current of the transformer and reduces the ripples in the output voltage due to phase shift of the secondary windings by 20 degrees. In addition, this system can set the voltage transfer ratio freely because the transformer is employed, although conventional matrix converters have limitation of the voltage transfer ratio.

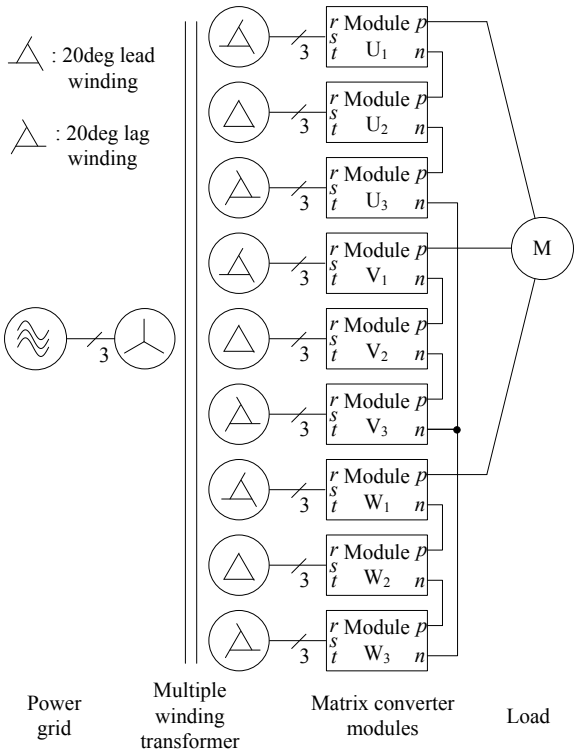

Fig. 1. System configuration of a series multi-modular matrix converter with nine matrix converter modules. A series multi-modular matrix converter provides high output voltage and multilevel waveform similar to sinusoidal.

Fig. 2 shows a simple model of a multi-modular matrix converter with single module per output phase for analysis and consideration. In Fig. 2, each module consists of a three-phase to single-phase matrix converter which controls output phase voltage and secondary current of the transformer. The bidirectional switch in the three-phase to single-phase matrix converter modules uses 2 series-connected IGBT-diode. Filter capacitors are connected closely with the bidirectional switches to mitigate surge voltage to the switches. An output terminal p is connected to load and another terminal n forms the neutral point with other modules.

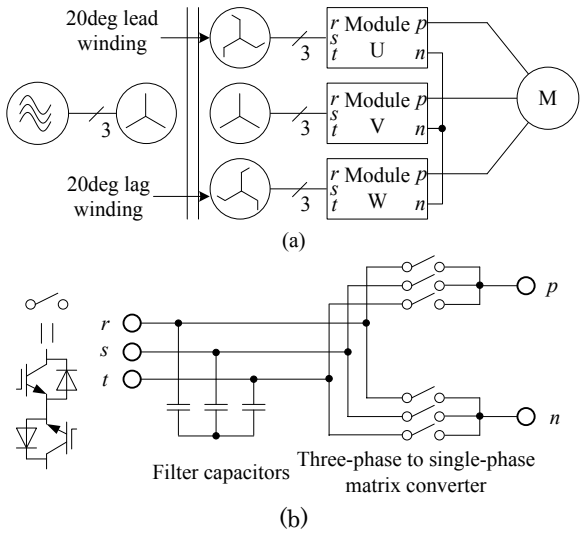

Fig. 2. Simple model of a multi-modular matrix converter with single module per output phase for analysis and consideration. (a) System configuration of a multi-modular matrix converter with three modules; (b) configuration of matrix converter modules which controls output phase voltage and secondary current of the transformer.

B. Mechanism of Filter Resonance

Fig. 3 shows the single-phase equivalent circuit of input filters of the multi-modular matrix converter as illustrated in Fig. 2. In Fig. 3, L_l is the leakage inductance of the transformer, C_f is the filter capacitor and R_{mcs} is the load resistance which consumes the steady power. Then, the input power factor is assumed to unity. Note that L_l, C_f and R_{mcs} are converted to the primary side of the transformer. In addition, the exciting reactance of the transformer is assumed to be much larger than the leakage inductance for the simplicity.

The filter resonance occurs because of an equivalent negative resistance which is virtually generated at a constant power load. The mechanism to generate the negative resistance will be described as follows.

First of all, the filter capacitor voltage v_c, the input current of multi-modular matrix converter i_{mc} and the output power p_{mc} are defined as follows.

$$v_c = v_{cs} + \Delta v_c \tag{1}$$

$$i_{mc} = i_{mcs} + \Delta i_{mc} \tag{2}$$

$$p_{mc} = p_{mcs} + \Delta p_{mc} \tag{3}$$

where, suffix s represents steady components based on the voltage source angular frequency ω_{in} whereas suffix Δ means differential components caused by transient state. Then, the steady components are expressed from (4) to (7).

$$v_{cs} = \sqrt{2} V_c \cos \omega_{in} t \tag{4}$$

$$i_{mcs} = \sqrt{2} I_{mc} \cos \omega_{in} t \tag{5}$$

$$p_{mcs} = v_{cs} i_{mcs} = V_c I_{mc} \left(1 + \cos 2\omega_{in} t\right) \tag{6}$$

$$R_{mcs} = \frac{v_{cs}}{i_{mcs}} = \frac{V_c}{I_{mc}} \tag{7}$$

where, V_c and I_{mc} are the RMS values of the filter capacitor voltage and input current of the multi-modular matrix converter. Note that the output power of the single-phase model oscillates with the frequency by twice of ω_{in} though the output power of three phase model is constant.

Then, from (1) to (3), i_{mc} is represented by (8).

$$i_{mc} = \frac{p_{mc}}{v_c} \tag{8}$$

Equation (8) is applied with the linear approximation method around the steady state operating point because (8) is a nonlinear equation. The input current i_{mc} is separated into steady and differential components and they are expressed as (9) and (10), respectively.

$$i_{mcs} = \frac{p_{mcs}}{v_{cs}} = \frac{1}{R_{mcs}} v_{cs} \tag{9}$$

$$\Delta i_{mc} = \frac{\Delta p_{mc} - \Delta v_c i_{mcs}}{v_{cs}} \tag{10}$$

For a constant load, Δp_{mc} becomes zero and (11) is derived.

$$\Delta i_{mc} = -\frac{i_{mcs}}{v_{cs}} \Delta v_c = -\frac{1}{R_{mcs}} \Delta v_c \tag{11}$$

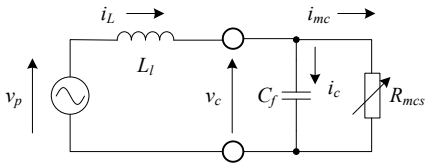

Fig. 3. Single-phase equivalent circuit of the input filters in the multi-modular matrix converter. The mechanism of the filter resonance is clarified using this equivalent circuit.

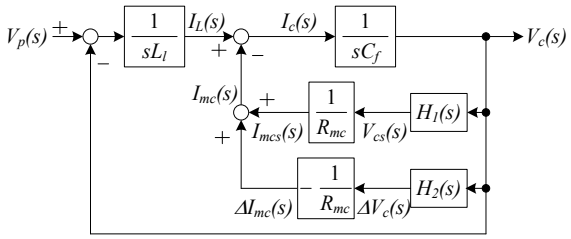

Fig. 4. Block diagram of a single-phase equivalent circuit of the input filters in the multi-modular matrix converter at constant load. $H_1(s)$ and $H_2(s)$ are the LPF and HPF respectively. This diagram has a positive feedback loop due to the equivalent negative resistance gain and becomes unstable with LC resonance.

Equation (11) indicates the fluctuation of the input current of the multi-modular matrix converter against the fluctuation of the filter capacitor voltage. In addition, an equivalent negative resistance is generated at a constant power control, which is obvious because the coefficient of Δv_c is a negative value.

Fig. 4 shows the block diagram of the single-phase equivalent circuit of input filters in the multi-modular matrix converter at constant load. In order to separate the steady and differential components, filters named $H_1(s)$ and $H_2(s)$ are introduced. $H_1(s)$ and $H_2(s)$ are the LPF (Low Pass Filter) and HPF (High Pass Filter) respectively, and defined by (12).

$$H_1(s) + H_2(s) = 1 \tag{12}$$

Then, Fig. 4 has a positive feedback loop because of the negative resistance gain $-1/R_{mc}$. As a result, this system becomes unstable with LC resonance. Therefore, the multi-modular matrix converter must cancel the negative resistance gain with its control strategy at a constant load.

III. Control Strategy to Suppress Filter Resonance

Fig. 5 shows the control block diagram of the multi-modular matrix converter employing the conventional active damping control. The basic concept of this technique is to insert a virtual harmonic damping resistor connected in parallel with the filter capacitor C_f owing to the input current control block in Fig. 5. As a result, the virtual harmonic damping resistor cancels the negative resistor with no influence on the fundamental component. However, the active damping control requires high speed response and high accurate voltage sensors in order to detect high frequency harmonic components. Besides, if the conventional active damping control is applied to the multi-modular matrix converter as illustrated in Fig. 5, the required voltage sensors

are increased with the number of modules, which is not cost effective. For example, the multi-modular matrix converter with nine modules as shown in Fig. 1 needs 18 voltage sensors at least for the active damping control. Therefore, the damping control for the multi-modular matrix converter which is independent from the voltage sensor is preferred.

In addition, as mentioned above, the conventional active damping control may be introduced to the input stage of the modules. On the other hand, for adjustable speed drive system of a motor, the current control is requited to the output stage of the multi-modular matrix converter when a vector control which composes ASR (Auto Speed Regulator) and ACR is implemented. Then, design of these controllers becomes complex because matrix converters have no energy buffers. Hence, the damping control which is combined with the output current control for a motor is preferred.

In order to overcome these issues, in this paper, the damping control combined to the output current control of the multi-modular matrix converter is proposed. The proposed method can divert the current sensors for ACR and does not require the voltage sensors at filter capacitors. Thus, the required sensors for the proposed damping control are independent from the number of modules. Furthermore, the design of controllers for ACR and damping control are simpler than the damping control in the input current control because the information of the controllers is collected to the output stage.

Fig. 6 shows the system block diagram of the multi-modular matrix converter with the proposed damping control. The matrix converter modules control the output voltage and the secondary current of the transformer at a same time. The output voltage control block includes a damping control to suppress the input filter resonance, and a vector control which is composed by ACR and ASR. On the other hand, the secondary current of the transformer is fed by open loop control. Then, the secondary voltage phase angles of the transformer θ_{2U}, θ_{2V} and θ_{2W} are calculated from (13) to (15) with the primary voltage phase angle of the transformer θ_1.

$$\theta_{2U} = \theta_1 + \pi/9 [rad] \tag{13}$$

$$\theta_{2V} = \theta_1 \tag{14}$$

$$\theta_{2W} = \theta_1 - \pi/9 [rad] \tag{15}$$

Next, this paragraph explains the output voltage control block. First of all, HPF which has a time constant T_{hpf} separates the harmonic components caused by the filter resonance from the output current, I_{dout} and I_{qout}. This is based on the principle that the resonant distortion appears in the output current since the matrix converters has no energy buffer. Then, the cut-off frequency of the HPF is set lower than the resonant frequency because the fundamental frequency component in the output current is converted to a constant value by a synchronous reference frame. Besides, the harmonic components are converted to ripples. Second, the extracted ripples are multiplied by the damping gain K_d, and subtracted from the output current. The above shows the theory of the damping control in order to suppress the resonant distortion. On the other hand, the output current is controlled by ACRs for the deviation obtained from the output current commands I_{dout}^* and I_{qout}^*, and feedback values from the damping control. Then, the damping control path becomes positive feedback eventually.

Fig. 7 shows the block diagram of a single-phase equivalent circuit of the input filters with the proposed damping control, where λ is the modulation index of the

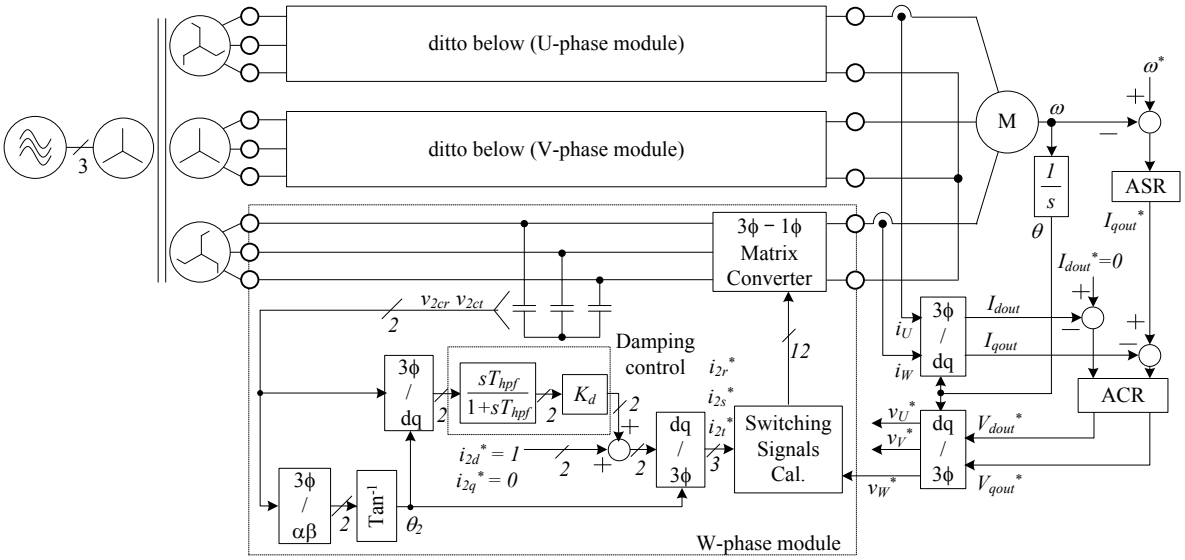

Fig. 5. Control block diagram of the multi-modular matrix converter employing the conventional active damping control. The active damping control to suppress the filter resonance is installed to input current control block. On the other hand, the output voltage control block has ACR for the output current and ASR for the motor speed. The damping control gain K_d behaves a virtual harmonic damping admittance in parallel with filter capacitors and suppress the filter resonance. However, the required voltage sensors for the conventional damping control increase with the number of modules.

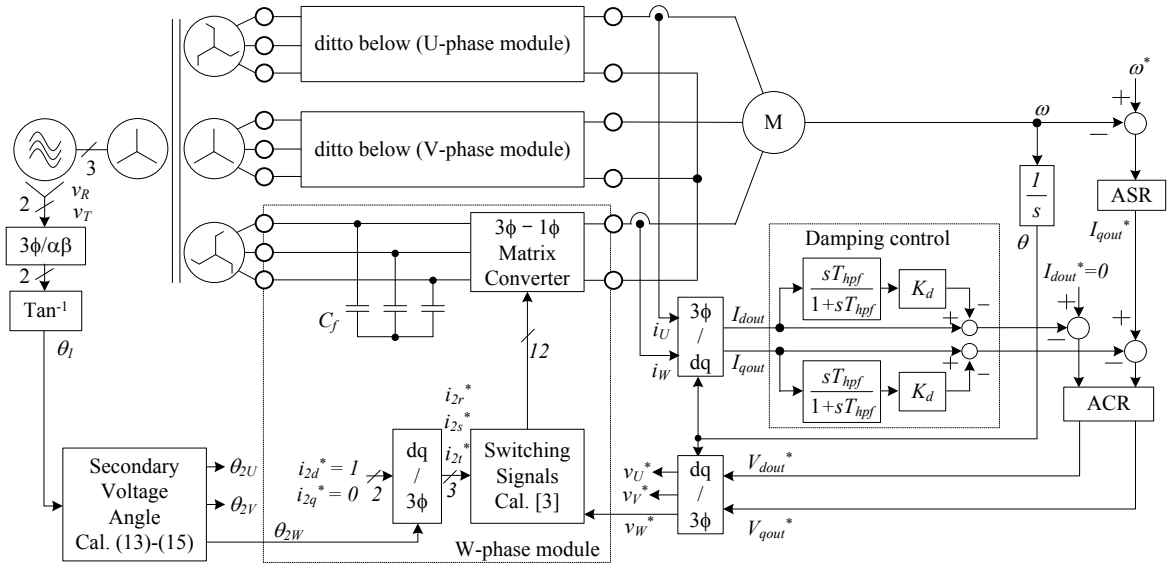

Fig. 6. Control block diagram of the multi-modular matrix converter with the proposed damping control. The output voltage control block includes a damping control to suppress the filter resonance, ACR and ASR for a vector control. In contrast, the secondary current control of the transformer is fed by open loop.

multi-modular matrix converter at steady state, I_{out}(s) is the output current, ΔI_{outd}(s) is the output of the damping control which subjects the ripples due to the resonance in Fig. 6, ΔV_{outd}(s) is the output of the PI controller regarding the resonant components, and ΔI_{mcd}(s) is the compensation value owing to the damping control. It is confirmed that the damping control loop is added in the filter block diagram. Then, the gain due to the damping control loop cancels the negative resistance gain which is the cause of the resonance because the damping control path is positive feedback in Fig. 6. Consequently, the system becomes stable and the filter resonance can be suppressed.

IV. Simulation Results

Table I presents simulation conditions for the multi-modular matrix converter with three modules drawn in Fig. 2. The simulation is tested with a vector control which is composed by the ASR and the ACR to control rotation speed of the IPM (Interior Permanent Magnetic) motor. The negative resistance appears because the ACR keeps constant output power in the motor load. In addition, note that the filter reactors are added instead of the large leakage inductance of a transformer. On the other hand, Table II shows the IPM motor parameters as the load in the simulation.

Fig. 8 shows the input and output waveforms of the multi-modular matrix converter at steady state in simulations. Note that these results are obtained when the IPM motor operates at rated speed and rated torque output. Fig. 8 (a) shows the result without damping controls and (b) shows the result with the proposed damping control. It can be confirmed that the primary current of the transformer contains large distortion caused by the filter resonance from Fig. 8 (a), and the primary current THD (Total Harmonic Distortion) is 62.9 %. Moreover, the output line voltage and the output current have large distortion too because matrix converter modules have no energy buffers. Then, the output current THD is 15.4 % from Fig. 8 (a). On the other hand, in Fig. 8 (b), the resonant distortion in the output current is mitigated by the proposed

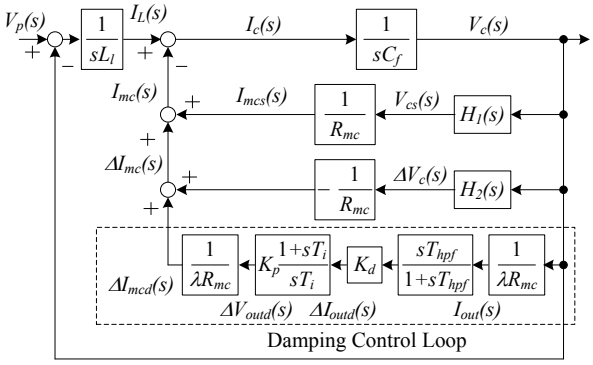

Fig. 7. Block diagram of the single-phase equivalent circuit of the input filters in the multi-modular matrix converter with the proposed damping control. This figure indicates a damping mechanism why the proposed damping control suppresses the filter resonance.

TABLE I. Simulation Conditions.

Input line voltage	200 V_{rms}	ASR natural frequency	63.7 Hz
Input frequency	50 Hz	ACR natural frequency	650 Hz
Rated power	3 kW	Carrier frequency	10 kHz
Trans. turn ratio	1	Damping gain	0.6 p.u.
Leakage inductance	9.42 %	Damping HPF cut off frequency	30 Hz
Input filter C	8.55 %		

TABLE II. IPM Motor Parameters.

Rated speed	1800 rpm (1 p.u.)
Rated line voltage	180 V_{rms}
Rated power	1.5 kW
Rated current	6.1 A_{rms} (1 p.u.)
d-axis inductance	11.5 mH
q-axis inductance	23.0 mH
Stator resistance	0.783 Ω
Inertia moment	0.00255 kgm^2

damping control. As a result, the input current contains less distortion compared to Fig. 8 (a). Both the primary current of the transformer and the output current THDs are under 1 % in Fig. 8 (b). In addition, the output line voltage obtains 5 levels waveform.

Fig. 9 shows the transient waveforms regarding the IPM motor. Fig. 9 (a) shows the result without damping controls and (b) shows the result with the proposed damping control. In Fig. 9 (a), the dq-axis currents and output torque oscillate during acceleration period and at rated speed and rated torque output due to the filter resonance. However, in Fig. 9 (b), the current and torque oscillations are suppressed by the proposed damping control. Then, the overshoot of the d-axis current by 1.2 p.u. occurs when the rated torque is provided although the d-axis current command is set to zero. This problem will be overcome by the optimal design of the controllers in future works. Therefore, it is confirmed from the simulation results that the proposed damping control suppresses the filter resonance and achieves stable operation with the IPM motor load.

V. Experimental Results

Table III presents experimental conditions for the multi-modular matrix converter with three modules drawn in Fig. 2. Note that the experiments are tested with a constant power load composed by a R-L load and the ACR, not a vector control. Then, the negative resistance appears even if the R-L load is used instead of the motor because the ACR keeps constant output power. In addition, the filter reactors are added instead of the large leakage inductance of a transformer in common with the simulation condition. Also, the voltage sensors in the filter capacitors are used because the commutation sequence based on the input voltage of the matrix converter are applied. However, the commutation sequence can be changed to a current type control using the output current, and the voltage sensors are not needed.

Fig. 10 shows the input and output waveforms of the multi-modular matrix converter obtained by the experiments. Fig. 10 (a) shows the result without damping controls and (b) shows the result with the proposed damping control. In Fig. 10 (a), the filter resonance is excited, and the primary current of the transformer and the output current have resonant distortions. In addition, the output line voltage is synthesized in over modulation region because the filter capacitor voltage is fluctuated by the filter resonance. Then, the primary current of the transformer and the output current THDs are obtained as follows, 20.1 % and 7.13 %. The reason that the current THDs measured from experiments are lower than the simulation results is that loss of the transformer and modules behave damping resistors. In contrast, the filter resonance is suppressed by the proposed damping control in Fig. 10 (b). Consequently, the input and output currents obtain lower distortion compared to Fig. 10 (a). Then, the primary current of the transformer and the output current THDs are 5.61 % and 2.62 %, respectively. Thus, the proposed damping control mitigates the resonance distortions by 72.1 %. Furthermore, the output line voltage obtains 5 levels waveform without the over modulation. Therefore, it is confirmed that the proposed

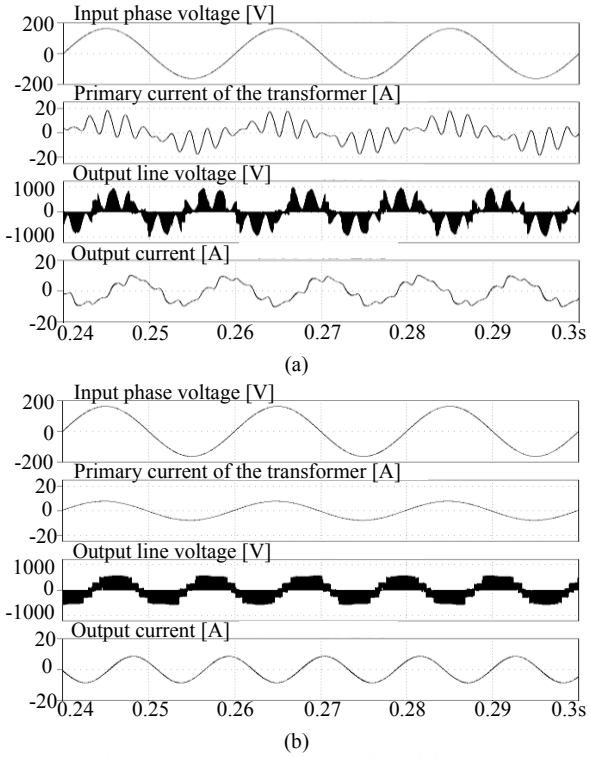

Fig. 8. Input and output waveforms of the multi-modular matrix converter as drawn in Fig. 2 at steady state in simulations. (a) Without damping controls which results in the primary current and the output current THDs by 62.9 % and 15.4 % respectively; (b) With the proposed damping control which results in the primary current and the output current THDs are under 1 %.

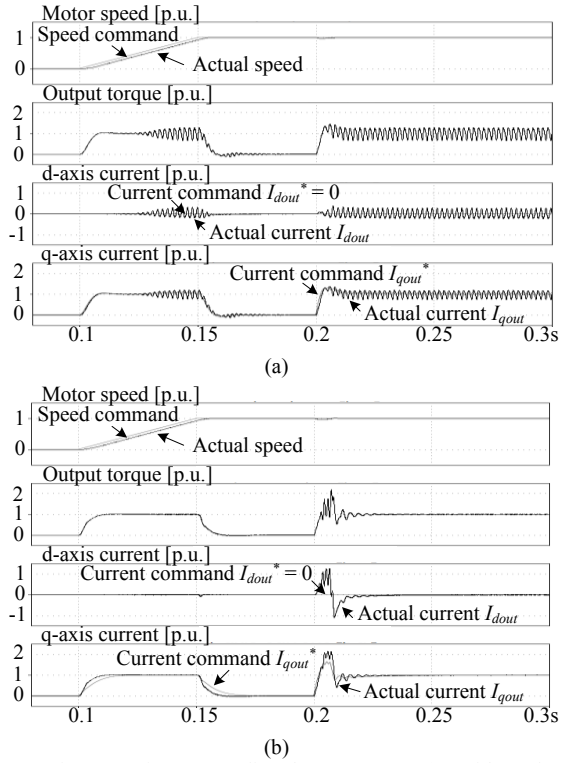

Fig. 9. Transient waveforms regarding the IPM motor. (a) Without damping controls which results in steady perturbation in the output torque and dq-axis currents due to the filter resonance; (b) With the proposed damping control which results in suppression of the steady fluctuation.

damping control suppresses the filter resonance and achieves stable operation.

Fig. 11 shows the harmonic components analysis of the primary current of the transformer. Fig. 11 (a) shows the result without the proposed damping control and (b) shows the result with the proposed control. In Fig. 11 (a), the primary current of the transformer includes the 340-Hz and 440-Hz components of approximately 10 % caused by the filter resonance. In contrast, in Fig. 11 (b), the resonant components are mitigated by the proposed damping control. In addition, the harmonic components within a range from 100-Hz to 1.25-kHz are suppressed by the proposed damping control since the control has low cut-off HPF (30-Hz). Then, the upper limit of suppressible harmonics is decided by the control bandwidth due to the carrier frequency.

Fig. 12 shows the THD characteristics obtained from the primary current of the transformer subjected to the load power. Note that the output line voltage is kept to 240-V_{rms} constantly. Without any damping controls, the primary current THD of the transformer is increased to approximately 20 % over 60 % load due to the resonance. On the other hand, the proposed damping control suppresses the THD under 7 % in the region more than 30 % load. Then, in the light load region especially under 20 % load, the proposed damping control cannot reduce the current THD because the main reason of increasing THD is caused by the small amplitude of the fundamental component of the primary current although the distortion components is almost constant unrelated to the load. Besides the distortion is caused by the commutation failure, is not caused by the filter resonance. Thus, the proposed damping control suppresses the resonant distortion in larger range of the output power.

Fig. 13 shows the THD characteristics of the primary current of the transformer subjected to the leakage inductance of the transformer. Without any damping controls, the primary current THD of the transformer increases with the leakage inductance. In particular, the data in the region over 10 % of the leakage inductance of the transformer could not be taken because the primary current of the transformer diverges due to the destabilization. However, the proposed damping control suppresses the primary current THD. Then, if the allowable THD is set to under 10 %, the proposed damping control can be applied to the condition which the leakage inductance of the transformer is under 14.1 %. Hence, the validity of the proposed damping control is confirmed in experiments.

TABLE III. EXPERIMENTAL CONDITIONS.

Input line voltage	200 V_{rms}	Output frequency	30 Hz
Input frequency	50 Hz	Load resistance	83.7 %
Rated power	3 kW	Load inductance	1.88 %
Trans. turn ratio	1	ACR natural frequency	650 Hz
Leakage inductance	9.42 %	Load current command	0.95 p.u.
Input filter C	8.55 %	Damping gain	0.6 p.u.
Carrier frequency	10 kHz	Damping HPF cut off frequency	30 Hz
Commutation time	2.5 μs		

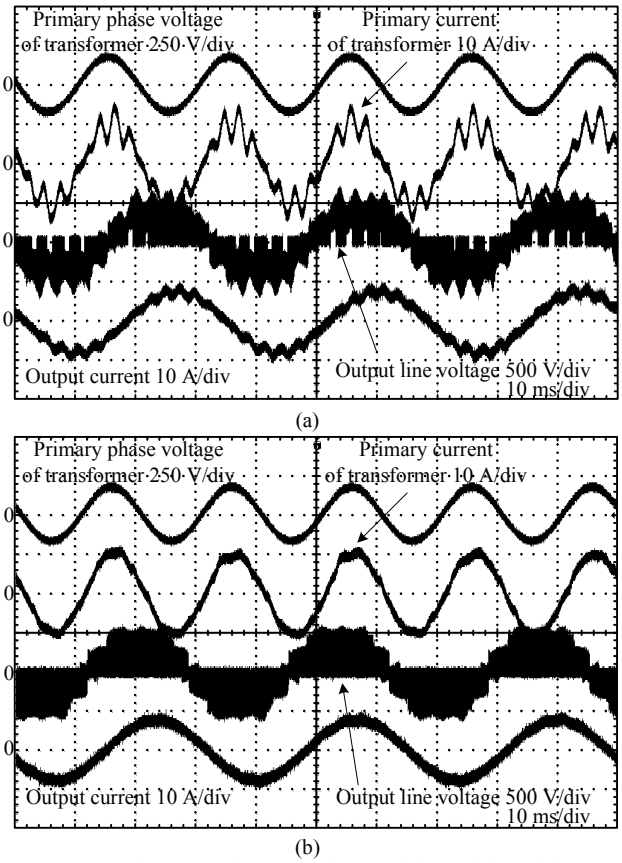

Fig. 10. Input and output voltage waveforms of the multi-modular matrix converter with three modules in experiments. (a) Without damping controls which results in the primary current THD and the output current THD by 20.1 % and 7.13 % respectively; (b) With the proposed damping control which results in the primary current THD and the output current THD by 5.61 % and 2.62 % respectively.

VI. CONCLUSION

This paper discusses the damping control to suppress the LC resonance caused from the input filter of the multi-modular matrix converter. Past works related to the damping control for current source converters and general matrix converters have not clarified the validity for the multi-modular matrix converter.

In this paper, a damping control suitable for the multi-modular matrix converter is proposed. The proposed damping control is combined to the output current control of the multi-modular matrix converter. Therefore, the proposed damping control suppresses the filter resonance and also diverts the output current sensors for ACR, which is generally used in adjustable speed drive system of a motor, instead of using high speed response voltage sensors on the input stage.

From simulation and experimental results, the multi-modular matrix converter without damping controls has large resonant distortion in the primary current of the transformer and the output current. However, the proposed damping control can mitigate the distortion by 72.1 % at steady state. In addition, from the THD characteristic of the primary current of the transformer which subjects to the load power, the

proposed control suppresses the THD under 7 % over 30 % load region. Moreover, the proposed damping control mitigates the resonant distortion under 7 % in conditions of the leakage inductance from 4.71 % to 14.1 %. Thus, the proposed damping control suppresses the filter resonant and the validity of the proposed control is confirmed in experiments.

REFERENCES

[1] P. W. Wheeler, J. Rodriguez, J. C. Clare, L. Empringham: "Matrix Converters: A Technology Review", IEEE Trans. Ind. Electron., Vol. 49, No. 2, pp. 274-288 (2002)

[2] T. Friedli, J. W. Kolar: "Milestones in Matrix Converter Research", IEEJ Journal I. A., Vol. 1, No. 1, pp. 2-14 (2012)

[3] J. Itoh, I. Sato, A. Odaka, H. Ohguchi, H. Kodachi, N. Eguchi: "A Novel Approach to Practical Matrix Converter Motor Drive System With Reverse Blocking IGBT", IEEE Trans. Power Electron., Vol. 20, No. 6, pp. 1356-1363 (2005)

[4] C. Klumpner, F. Blaabjerg, I. Boldea, P. Nielsen: "New Modulation Method for Matrix Converters", IEEE Trans. Ind. Appl., Vol. 42, No. 3, pp. 797-806 (2006)

[5] F. Blaabjerg, D. Casadei, C. Klumpner, M. Matteini: "Comparison of Two Current Modulation Strategies for Matrix Converters Under Unbalanced Input Voltage Conditions", IEEE Trans. Ind. Electron., Vol. 49, No. 2, pp. 289-296 (2002)

[6] M. Rivera, J. Rodriguez, J. Espinoza, T. Friedli, J. W. Kolar, A. Wilson, C. A. Rojas: "Imposed Sinusoidal Source and Load Currents for an Indirect Matrix Converter", IEEE Trans. Ind. Electron., Vol. 59, No. 9, pp. 3427-3435 (2012)

[7] J. W. Kolar, T. Friedli, F. Krismer, S. D. Round: "The Essence of Three-Phase AC/AC Converter Systems", Proc. 13th Power Electronics and Motion Control Conf., Vol. , No. , pp. 27-42 (2008)

[8] J. Kang, E. Yamamoto, M. Ikeda, E. Watanabe: "Medium-Voltage Matrix Converter Design Using Cascaded Single-Phase Power Cell Modules", IEEE Trans. Ind. Electron., Vol. 58, No. 11, pp. 5007-5013 (2011)

[9] E. Yamamoto, H. Hara, T. Uchino, M. Kawaji, T. J. Kume, J. K. Kang, H. P. Krug: "Development of MCs and its Applications in Industry", IEEE Industrial Electronics Magazine, Vol. 5, No. 1, pp. 4-12 (2011)

[10] J. Wang, B. Wu, D. Xu, N. R. Zargari: "Multimodular Matrix Converters With Sinusoidal Input and Output Waveforms", IEEE Trans. Ind. Electron., Vol. 59, No. 1, pp. 17-26 (2012)

[11] D. Casadei, G. Serra, A. Tani, A. Trentin, L. Zarri: "Theoretical and Experimental Investigation of the Stability of Matrix Converters", IEEE Trans. Ind. Electron., Vol. 52, No. 5, pp. 1409-1419 (2005)

[12] J. C. Wiseman, B. Wu: "Active Damping Control of a High-Power PWM Current-Source Rectifier for Line-Current THD Reduction", IEEE Trans. Ind. Electron., Vol. 52, No. 3, pp. 758-764 (2005)

[13] Y. W. Li: "Control and Resonance Damping of Voltage-Source and Current-Source Converters With LC Filters", IEEE Trans. Ind. Electron., Vol. 56, No. 5, pp. 1511-1521 (2009)

[14] Y. W. Li, B. Wu, N. R. Zargari, J. C. Wiseman, D. Xu: "Damping of PWM Current-Source Rectifier Using a Hybrid Combination Approach", IEEE Trans. Power Electron., Vol. 22, No. 4, pp. 1383-1393 (2007)

[15] M. Rivera, C. Rojas, J. Rodriguez, P. W. Wheeler, B. Wu, J. Espinoza: "Predictive Current Control With Input Filter Resonance Mitigation for a Direct Matrix Converter", IEEE Trans. Power Electron., Vol. 26, No. 10, pp. 2794-2803 (2011)

[16] J. Haruna, J. Itoh: "A Control Strategy for a Matrix Converter under a Large Impedance Power Supply", Proc. PESC 2007, pp. 659-664 (2007)

[17] J. Haruna, J. Itoh: "Control Strategy for a Matrix Converter with a Generator and a Motor", Proc. 26th IEEE APEC, pp. 1782-1789 (2011)

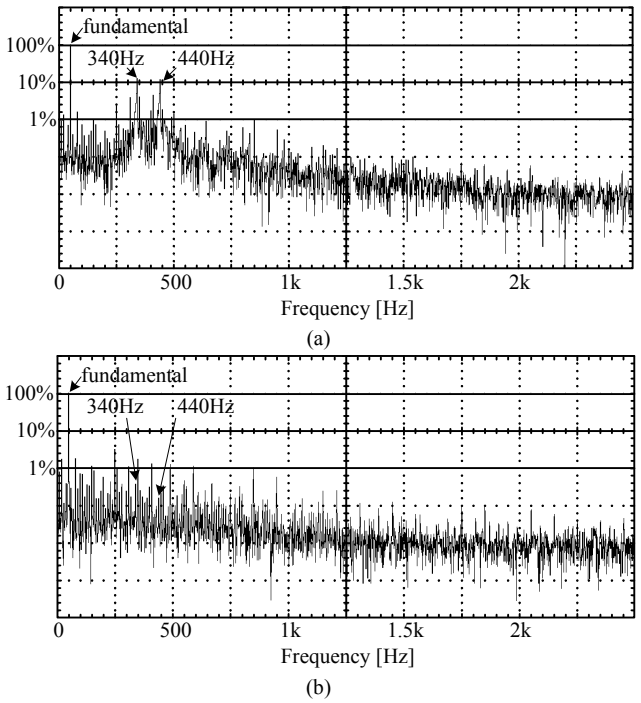

Fig. 11 Spectrum of the primary current of transformer with experiments. (a) Without damping controls; (b) With the proposed damping control. In (a), 340-Hz and 440-Hz components caused by the filter resonance are included. However, these components can be reduced in (b) by the proposed control.

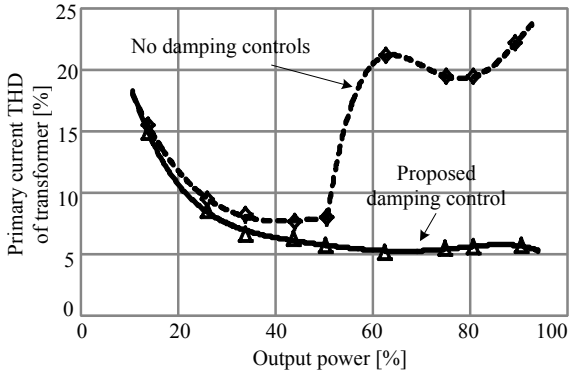

Fig. 12. THD characteristics obtained from the primary current of the transformer subjected to the load power. The proposed damping control reduces the resonant distortion under 7 % over 30 % load region.

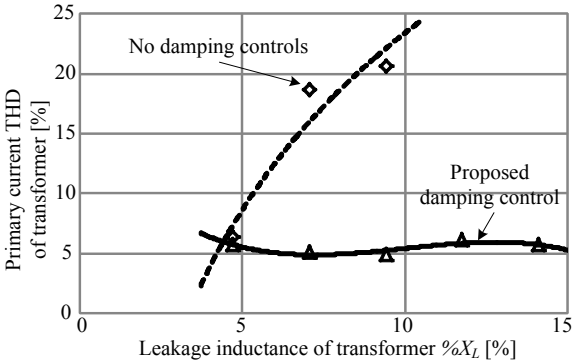

Fig. 13. THD characteristics of the primary current of the transformer subjected to the leakage inductance of the transformer. The proposed damping control mitigates the resonant distortion under 7% in entire range of the leakage inductance of the transformer.